

Electronic properties of graphene stacks.

A. Castro-Neto (Boston U.)

N. M. R. Peres (U. Minho, Portugal)

E. V. Castro, J. dos Santos (Porto), J. Nilsson (BU), A. Morpurgo (Delft), D. Huertas-Hernando (Trondheim), J. González, F. G., M. P. López-Sancho, T. Stauber, M. A. H. Vozmediano, B Wunsch (CSIC, Madrid)

Outline

- Electronic structure of graphite.
- Electron-electron interaction in graphene.
- Graphene stacks. Interlayer coupling.
- Electronic structure.
- Interaction effects.
- Disorder. Out of plane conductivity.
- Screening and surfaces.
- Transport in curved graphene sheets.
- Weak antilocalization effects.

Some interesting references

Electric Field Effect in Atomically Thin Carbon Films

K. S. Novoselov,¹ A. K. Geim,^{1*} S. V. Morozov,² D. Jiang,¹
Y. Zhang,¹ S. V. Dubonos,² I. V. Grigorieva,¹ A. A. Firsov²

We describe monocrystalline graphitic films, which are a few atoms thick but are nonetheless stable under ambient conditions, metallic, and of remarkably high quality. The films are found to be a two-dimensional semimetal with a tiny overlap between valence and conduction bands, and they exhibit a strong ambipolar electric field effect such that electrons and holes in concentrations up to 10^{13} per square centimeter and with room-temperature mobilities of $\sim 10,000$ square centimeters per volt-second can be induced by applying gate voltage.

The ability to control electronic properties of a material by externally applied voltage is at the heart of modern electronics. In many cases, it is the electric field effect that allows one to vary the carrier concentration in a semiconductor device and, consequently, change an electric current through it. As the

semiconductor industry is nearing the limits of performance improvements for the current technologies dominated by silicon, there is a constant search for new, nontraditional materials whose properties can be controlled by the electric field. The most notable recent examples of such materials are organic conductors (1) and carbon nanotubes (2). It has long been tempting to extend the use of the field effect to metals [e.g., to develop all-metallic transistors that could be scaled down to much smaller sizes and would consume less energy and operate at higher frequencies

than traditional semiconducting devices (3)]. However, this would require atomically thin metal films, because the electric field is screened at extremely short distances (< 1 nm) and bulk carrier concentrations in metals are large compared to the surface charge that can be induced by the field effect. Films so thin tend to be thermodynamically unstable, becoming discontinuous at thicknesses of several nanometers; so far, this has proved to be an insurmountable obstacle to metallic electronics, and no metal or semimetal has been shown to exhibit any notable ($> 1\%$) field effect (4).

We report the observation of the electric field effect in a naturally occurring two-dimensional (2D) material referred to as few-layer graphene (FLG). Graphene is the name given to a single layer of carbon atoms densely packed into a benzene-ring structure, and is widely used to describe properties of many carbon-based materials, including graphite, large fullerenes, nanotubes, etc. (e.g., carbon nanotubes are usually thought of as graphene sheets rolled up into nanometer-sized cylinders) (5–7). Planar graphene itself has been presumed not to exist in the free state, being unstable with respect to the formation of curved structures such as soot, fullerenes, and nanotubes (5–14).

¹Department of Physics, University of Manchester, Manchester M13 9PL, UK. ²Institute for Microelectronics Technology, 142432 Chernogolovka, Russia.

*To whom correspondence should be addressed. E-mail: geim@man.ac.uk

Single layer graphene.
Electrically doped.

Two-dimensional atomic crystals

K. S. Novoselov*, D. Jiang*, F. Schedin*, T. J. Booth*, V. V. Khotkevich*, S. V. Morozov[†], and A. K. Geim*[‡]

*Centre for Mesoscience and Nanotechnology and School of Physics and Astronomy, University of Manchester, Manchester M13 9PL, United Kingdom; and [†]Institute for Microelectronics Technology, Chernogolovka 142432, Russia

Edited by T. Maurice Rice, Swiss Federal Institute of Technology, Zurich, Switzerland, and approved June 7, 2005 (received for review April 6, 2005)

And more interesting references

Vol 438|10 November 2005|doi:10.1038/nature04233

nature

LETTERS

Two-dimensional gas of massless Dirac fermions in graphene

K. S. Novoselov¹, A. K. Geim¹, S. V. Morozov², D. Jiang¹, M. I. Katsnelson³, I. V. Grigorieva¹, S. V. Dubonos² & A. A. Firsov²

Vol 438|10 November 2005|doi:10.1038/nature04235

nature

LETTERS

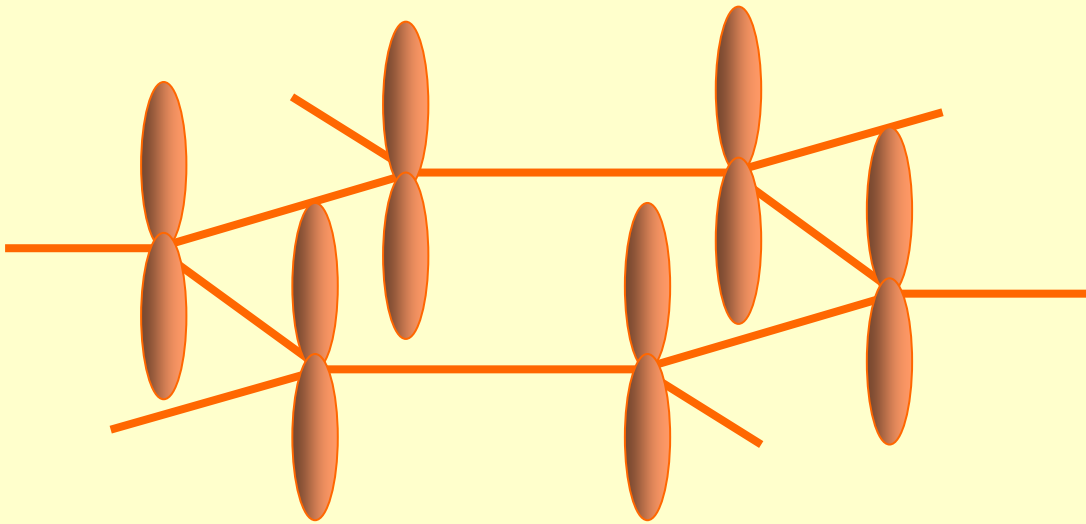
Experimental observation of the quantum Hall effect and Berry's phase in graphene

Yuanbo Zhang¹, Yan-Wen Tan¹, Horst L. Stormer^{1,2} & Philip Kim¹

Integer Quantum Hall effect in graphene.

Electronic band structure

J. W. McClure, Phys. Rev. **108**, 612 (1957)



-The conduction band is built up from the unpaired π orbitals at the C atoms.

-The crystal structure is stabilized by the σ bonds within the plane.

-The hybridization between π orbitals in neighbouring planes cannot be neglected.

Hybridization between in plane nearest neighbours: $\gamma_0 \approx 2.4\text{eV}$

Hybridization between out of plane nearest neighbours: $\gamma_1 \approx 0.3\text{eV}$

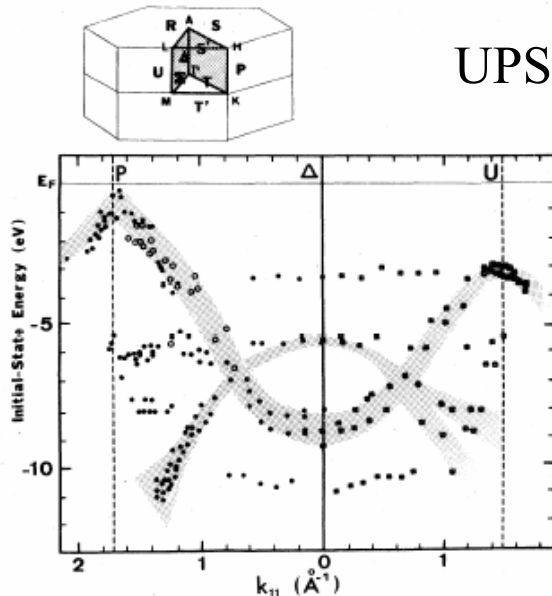
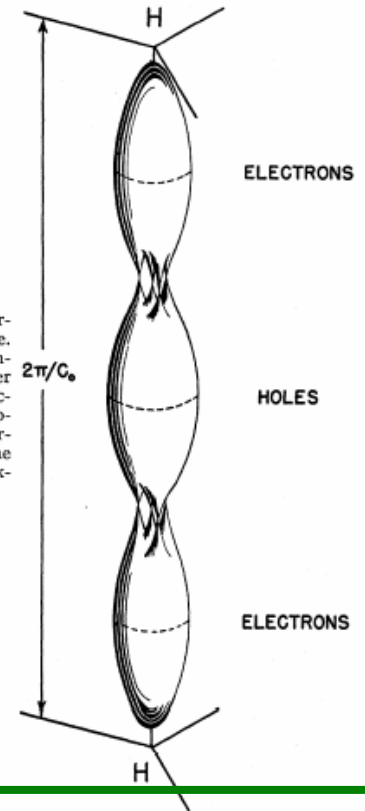
Electronic band structure

D. E. Soule, J. W. McClure, and L. B. Smith, *Phys. Rev.* **134**, A454 (1964).

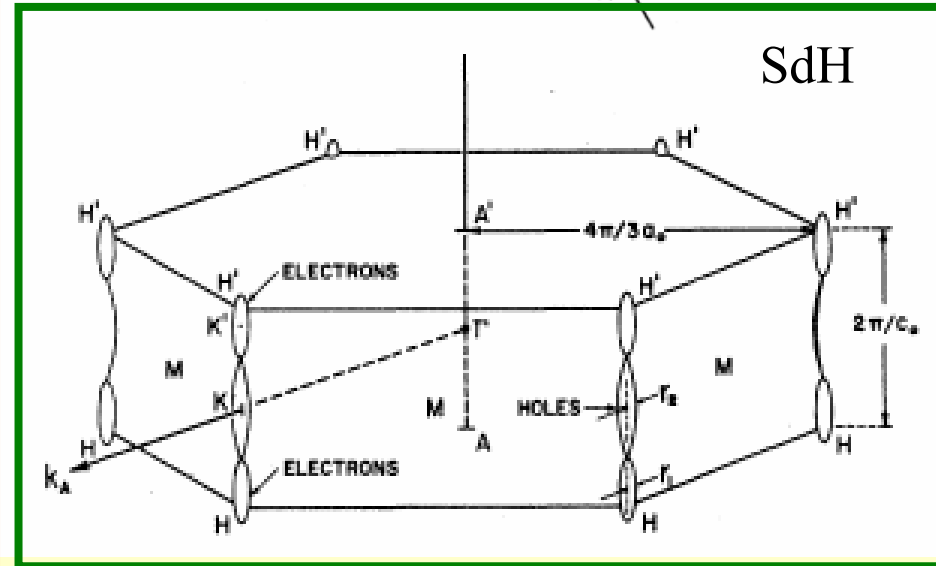
D. Marchand, C. Fréty, M. Lagües, F. Batallan, Ch. Simon, I. Roseman, and R. Pinchaux, *Phys. Rev. B* **30**, 4788 (1984).

The Fermi surface has electron and hole like pockets at the edges of the Brillouin zone.
 The effective masses are small, $m_{\text{eff}} \approx 0.06m_0$
 The structure is consistent with Shubnikov-de Haas and photoemission experiments.

FIG. 4. The Fermi surface for pure graphite. The central surface contains holes and the outer surfaces contain electrons. The length-to-width ratio of each surface is about 13. The trigonal anisotropy is exaggerated for clarity.



UPS

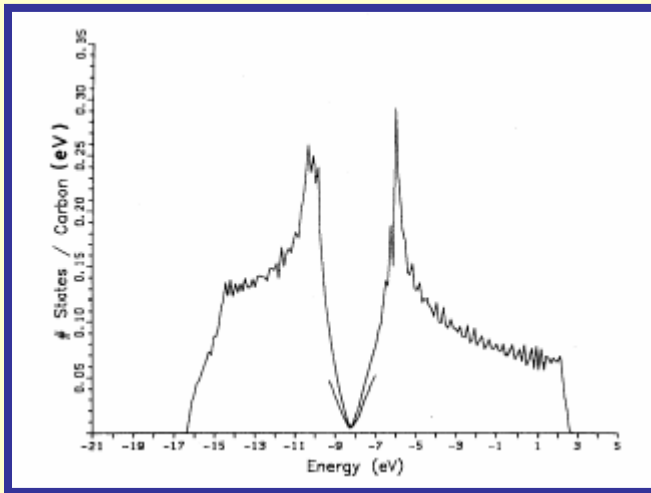


SdH

Electronic band structure

R. C. Tatar, and S. Rabii, Phys. Rev. B **25**, 4126 (1982).

J.-C. Charlier, X. Gonze, and J.-P. Michenaud, Phys. Rev. B **43**, 4579 (1991).



Graphite is a semimetal.

$$N(\epsilon_F) \approx 1.2 \times 10^{-4} \text{ states}/(\text{eV C atom})$$

$$n \approx 2.4 \times 10^{18} \text{ cm}^{-3}$$

$$\lambda_{\text{FT}} \approx 50 \text{ nm}$$

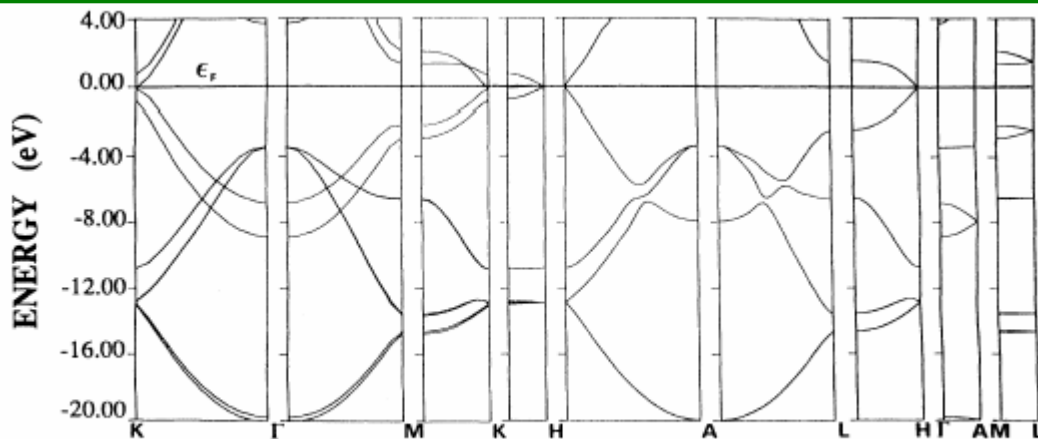
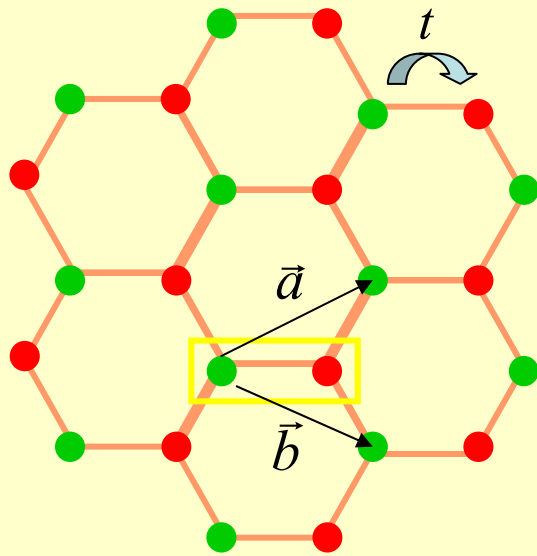


FIG. 3. *Ab initio* band structure of graphite along different lines in the Brillouin zone.

A graphene plane. The Dirac equation.



$$H = t \sum_{n.n.} c_{i,s}^+ c_{j,s} + h.c.$$

$$H_{\vec{k}} \equiv \begin{pmatrix} 0 & t(1 + e^{-i\vec{k}\vec{a}} + e^{-i\vec{k}\vec{b}}) \\ t(1 + e^{i\vec{k}\vec{a}} + e^{i\vec{k}\vec{b}}) & 0 \end{pmatrix}$$

$$\varepsilon_{\vec{k}} = \pm t \sqrt{3 + 2 \cos(\vec{k}\vec{a}) + 2 \cos(\vec{k}\vec{b}) + 2 \cos[\vec{k}(\vec{a} - \vec{b})]}$$

$$\vec{k} = \vec{k}_0 + \delta \vec{k}$$

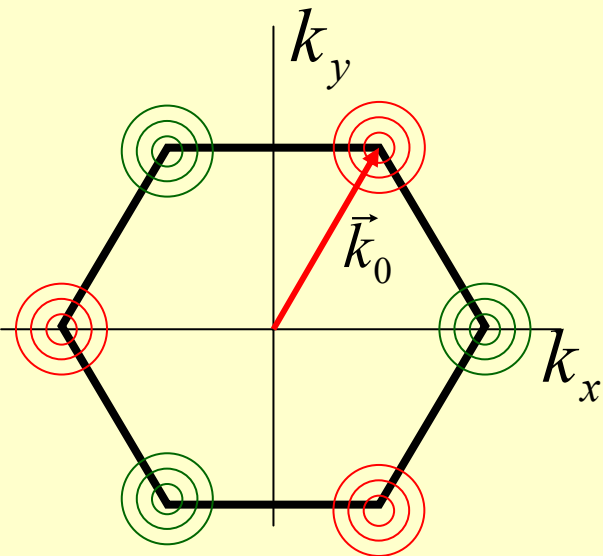
$$\vec{k}_0 = \frac{4\pi}{3\sqrt{3}a} \begin{pmatrix} 1 \\ 2 \\ \sqrt{3} \\ 2 \end{pmatrix}$$

$$\vec{a} = a\sqrt{3}(1,0)$$

$$\vec{b} = a\sqrt{3} \begin{pmatrix} 1 \\ 2 \\ \sqrt{3} \\ 2 \end{pmatrix}$$

$$e^{i\vec{k}_0\vec{a}} = -\frac{1}{2} + i\frac{\sqrt{3}}{2}$$

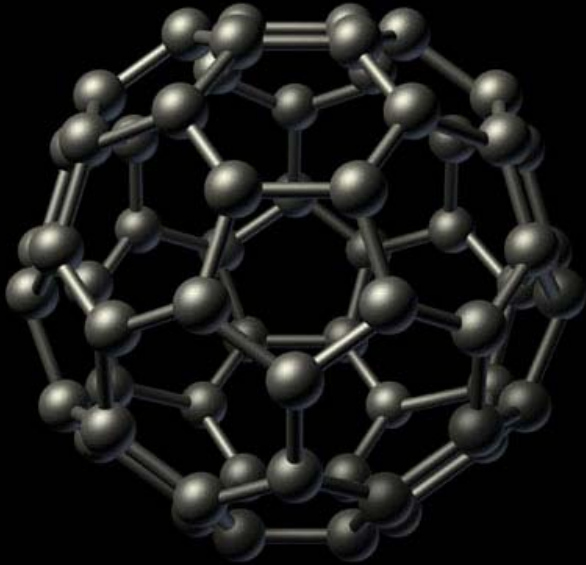
$$e^{i\vec{k}_0\vec{b}} = -\frac{1}{2} - i\frac{\sqrt{3}}{2}$$



Dirac equation:

$$H \cong \frac{3ta}{2} \begin{pmatrix} 0 & k_x + ik_y \\ k_x - ik_y & 0 \end{pmatrix}$$

Related systems. C_{60}

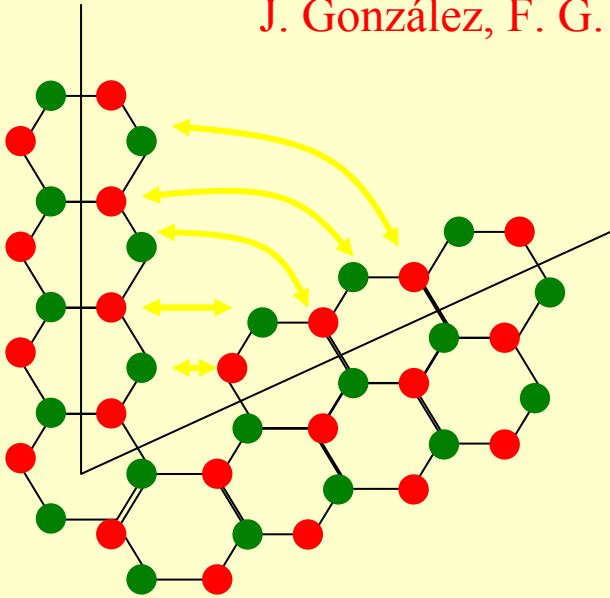


- **Threefold coordination**
- **The curvature is induced by five-fold rings**
- **There is a family of quasispherical compounds**
- **The valence orbitals are derived from π atomic orbitals.**

The Dirac equation on a sphere?

Lattice frustration as a gauge potential.

J. González, F. G. and M. A. H. Vozmediano, Phys. Rev. Lett. **69**, 172 (1992)



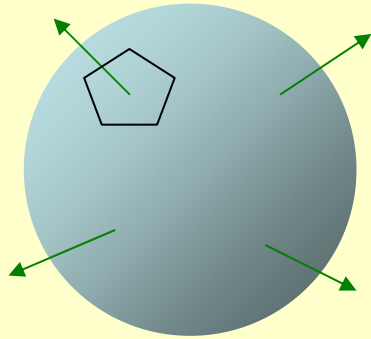
- A fivefold ring defines a disclination.
- The sublattices are interchanged.
- The Fermi points are also interchanged.
- These transformations can be achieved by means of a gauge potential.

$$i\vec{\nabla} \rightarrow i\vec{\nabla} - \vec{A} \begin{pmatrix} 0 & 1 \\ 1 & 0 \end{pmatrix}$$

$$\Phi = \int \vec{A} d\vec{l}$$

The flux Φ is determined by the total rotation induced by the defect.

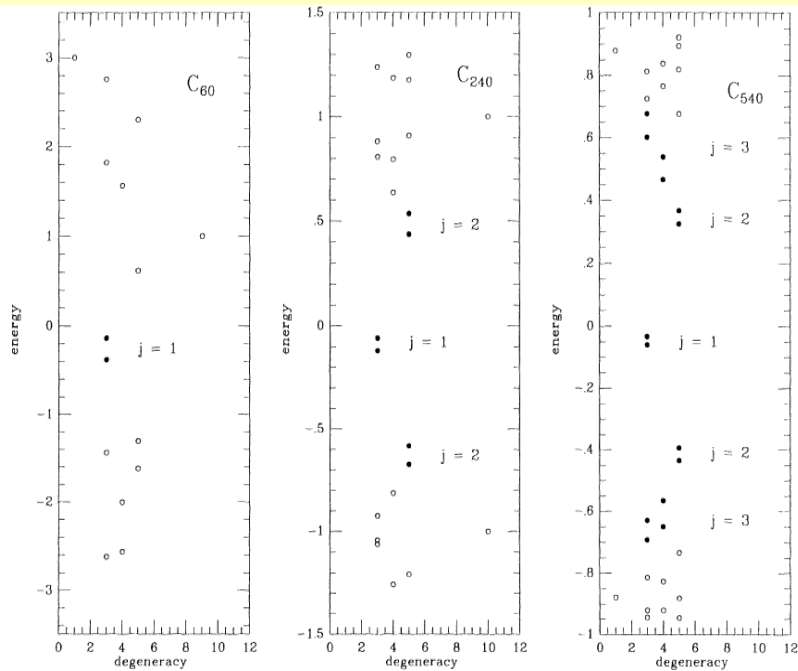
Continuum model of the fullerenes.



- Dirac equation on a spherical surface.
- Constant magnetic field (**Dirac monopole**).

$$\frac{\hbar v_F}{R} \left[i\partial_\theta - \frac{1}{\sin(\theta)} \partial_\phi + \frac{i(1+l)\cos(\theta)}{2\sin(\theta)} \right] \Psi_a = \varepsilon \Psi_b$$

$$\frac{\hbar v_F}{R} \left[i\partial_\theta + \frac{1}{\sin(\theta)} \partial_\phi + \frac{i(1-l)\cos(\theta)}{2\sin(\theta)} \right] \Psi_b = \varepsilon \Psi_a$$



$$\varepsilon_J = \frac{\hbar v_F}{R} \sqrt{[J(J+1)] - l(l+1)} \quad J \geq l$$

Coulomb interactions

Non Fermi liquid behavior of quasiparticle lifetimes.

Expts: S. Yu, J. Cao, C. C. Miller, D. A. Mantell, R. J. D. Miller, and Y. Gao, Phys. Rev. Lett. **76**, 483 (1996).

Theory: J. González, F. G., and M. A. H. Vozmediano Phys. Rev. Lett. **77**, 3589 (1996)

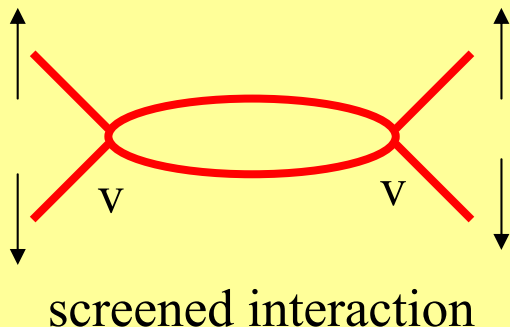
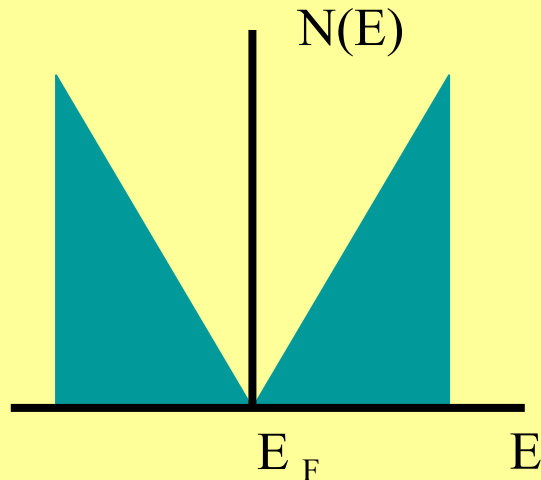
Single graphene planes:

- Absence of screening.
- Perturbation theory leads to logarithmic divergences.
- The expansion has similar properties to that for 1D metallic systems (Luttinger liquids).
- Large coupling constant: $e^2/v_F=2-5$
- Deviations from Fermi liquid behavior.

Limits of validity:

High energies $> 0.3\text{eV}$.

Neglects electron-phonon interaction.



Renormalization of the Coulomb interaction.

$$H = iv_F \int d^2\vec{r} \Psi^\dagger(\vec{r}) \sigma \cdot \vec{\nabla} \Psi(\vec{r}) + \\ + \frac{e^2}{8\pi} \iint d^2\vec{r}_1 d^2\vec{r}_2 \Psi^\dagger(\vec{r}_1) \Psi(\vec{r}_1) \frac{1}{|\vec{r}_1 - \vec{r}_2|} \Psi^\dagger(\vec{r}_2) \Psi(\vec{r}_2)$$

Dimensional analysis:

$$[l] \equiv [t]$$

$$[H_K] \equiv [H_{int}] \equiv \frac{1}{l}$$

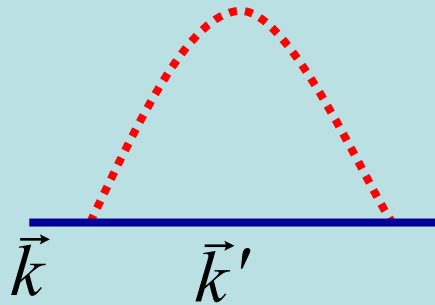
$$[\Psi] \equiv \frac{1}{l^{D/2}}$$

$$[e^2] \equiv l^0$$

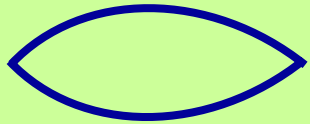
- The interaction is marginal in any dimension (as in QED).
- The interaction is mediated by photons in three dimensional space.
- The interaction breaks the Lorentz invariance of the Dirac equation.

Renormalization of the Coulomb interaction.

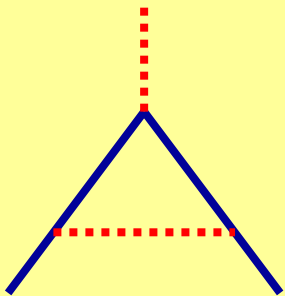
J. González, F. G. and M. A. H. Vozmediano., Nucl. Phys. B **424**, 595 (1994)



Hartree Fock selfenergy:
$$\Sigma(\vec{k}) \approx \frac{e^2}{8\pi} \vec{\sigma} \vec{k} \log\left(\frac{\Lambda}{|\vec{k}|}\right)$$

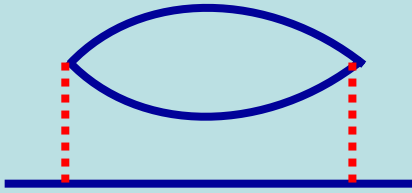


Bare polarizability:
$$\Pi_0(\vec{k}, \omega) = i \frac{e^2}{8} \frac{\vec{k}^2}{\sqrt{v_F^2 \vec{k}^2 - \omega^2}}$$



The vortex corrections are finite (to all orders).

Renormalization of the Coulomb interaction.



One loop calculation:
Renormalization of the
particle residue.

$$\Psi_R = Z^{-1/2} \Psi_0$$

$$Z^{-1} = \frac{\partial \Sigma}{\partial \omega}$$

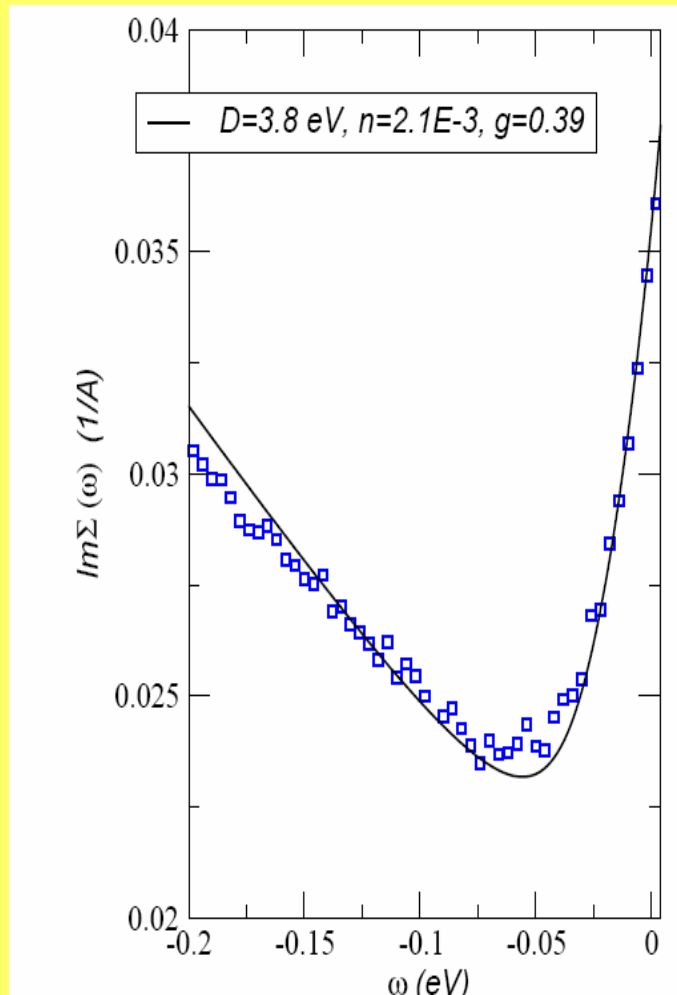
$$\text{Im} \Sigma(\omega) \propto |\omega|$$

Lowest order RG flow:

$$\Lambda \frac{\partial}{\partial \Lambda} \frac{e^2}{v_F} = \frac{8}{\pi^2} \frac{e^2}{v_F}$$

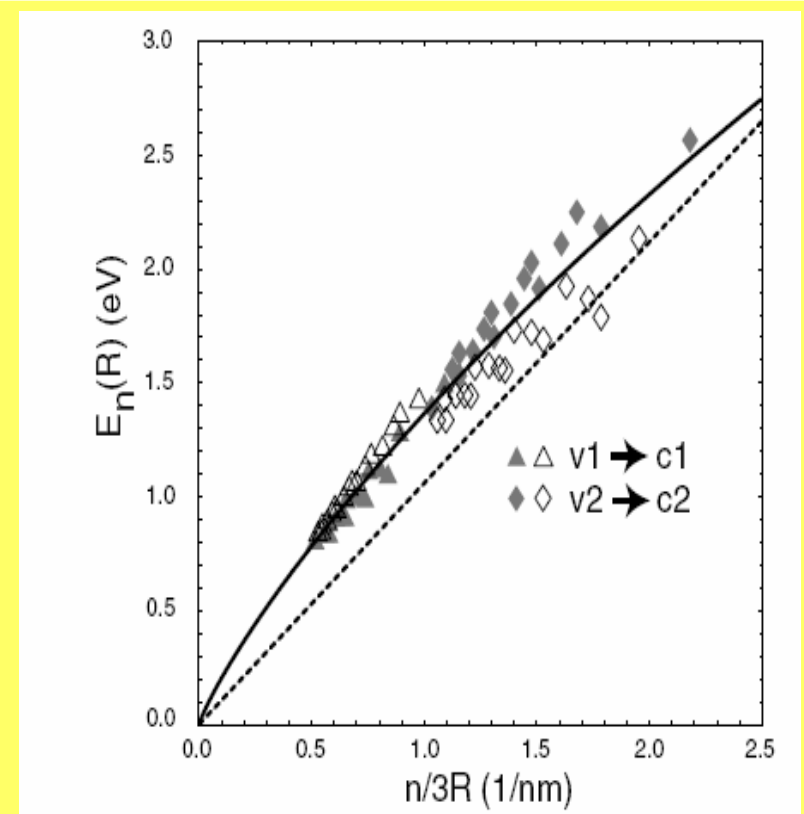
The coupling constant goes to zero at low energies.

Experimental consequences?



A. Lanzara *et al*, unpublished.

The combined effects of disorder and electron-electron interactions lead to a non monotonous dependence of the quasiparticle lifetime on disorder.



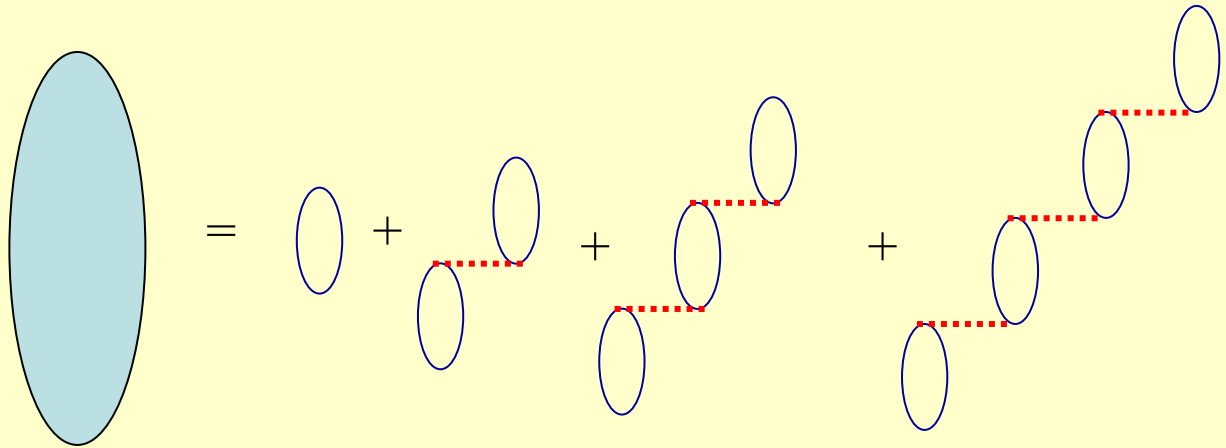
C. L. Kane and E. J. Mele, *Phys. Rev. Lett.* **93**, 197402 (2004)

The electronic self energy due to the long range Coulomb interaction modifies the dependence of the gap on the radius in semiconducting nanotubes.

Renormalization of the Coulomb interaction.

J. González, F. G. and M. A. H. Vozmediano, Phys. Rev. B **59**, R2474 (1999)

RPA summation:



RG flow equation:

(which can be analytically
extended to $g > 1$)

$$\Lambda \frac{\partial}{\partial \Lambda} g = \frac{8}{\pi^2} \left(g + \frac{\arccos g}{\sqrt{1-g^2}} \right) - \frac{4}{\pi}$$

The coupling constant always flows to zero at low energies.

Non perturbative phase transitions.

D.V. Khveshchenko, Phys. Rev. Lett. **87**, 246802 (2001).

Compensation between low density of states and unscreened interaction

Stoner criterium:

$$U_c N(E_F) = 1 \quad \leftrightarrow \quad N_f \frac{e^2}{|\vec{q}|} \frac{|\vec{q}|}{v_F} = 1$$

For sufficiently large couplings, a charge density wave phase is induced

Interlayer hopping

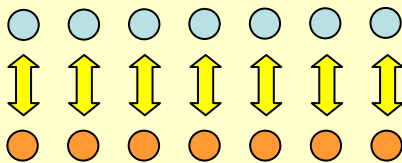
M. A. H. Vozmediano, M. P. López-Sancho, and F. G., Phys. Rev. Lett. **89**, 166401 (2002); *ibid*, Phys. Rev. B **68**, 195122 (2003).



In plane interactions reduce the interlayer coupling.
Similar effect as in the cuprate superconductors.

Interchain hopping in Luttinger liquids

Extended hopping



X.G. Wen, Phys. Rev. B **42**, 6623 (1990).

F. G. and G. Zimanyi, Phys. Rev. B **47**, 501 (1993).

S. Chakravarty and P.W. Anderson, Phys. Rev. Lett. **72**, 3859 (1994).

J.M.P. Carmelo, P.D. Sacramento, and F. G., Phys. Rev. B **55**, 7565 (1987)

A.H. Castro-Neto and F. G., Phys. Rev. Lett. **80**, 4040 (1998).

See also:

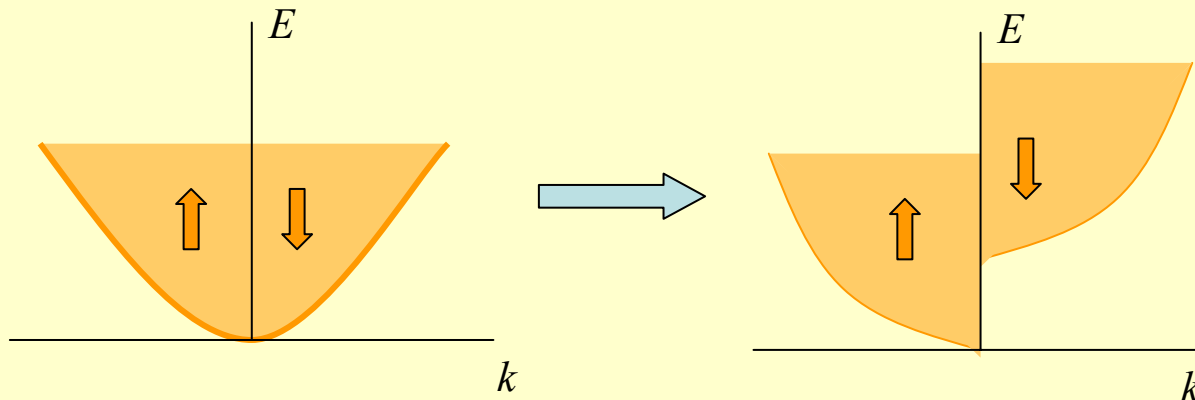
Local hopping



C.L. Kane and M.P.A. Fisher, Phys. Rev. Lett. **68**, 1220 (1992)

Exchange instability in graphene.

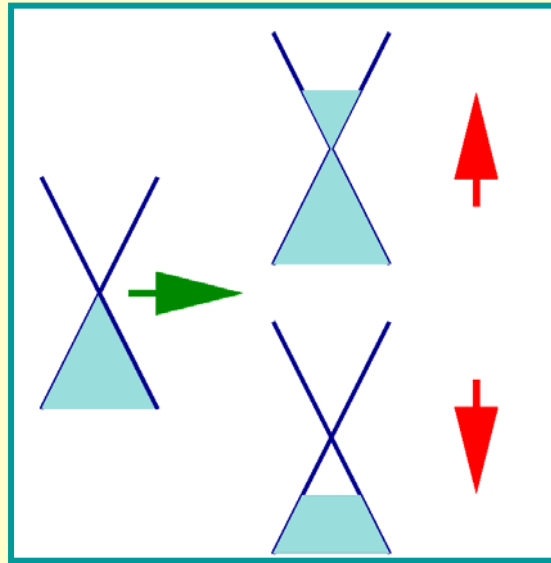
N. M. R. Peres, F. G. and A. H. Castro Neto, Phys. Rev. B 72, 174406 (2005)



$$E(k_{\uparrow}, k_{\downarrow}) = \underbrace{\frac{A \hbar^2}{4\pi 2m} (k_{\uparrow}^4 + k_{\downarrow}^4)}_{\text{Kinetic energy}} + \underbrace{\frac{A e^2 8}{4\pi^2 2\epsilon_0 3} (k_{\uparrow}^3 + k_{\downarrow}^3)}_{\text{Exchange energy}}$$

The exchange energy favors a ferromagnetic ground state.
This instability is expected in a low density 2DEG.

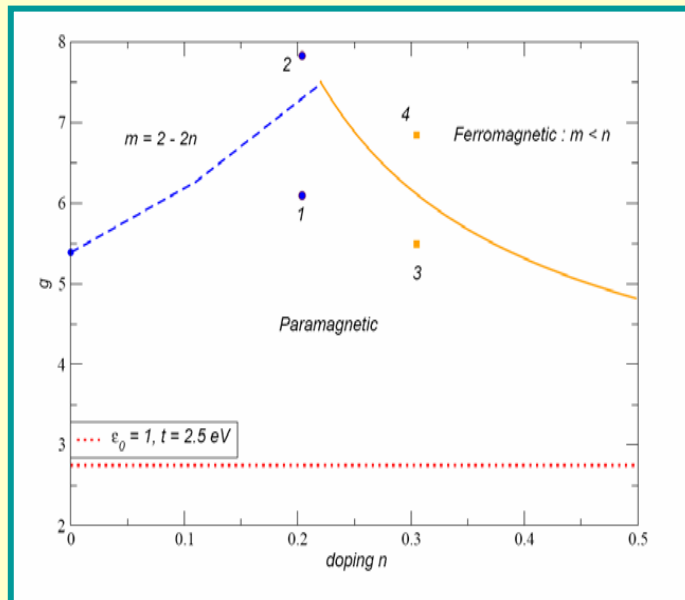
Exchange instability in graphene.



The interband exchange energy increases.

The intraband exchange energy decreases.

There is a competition between the two effects.



The instability requires too high coupling values.

$$g = \frac{e^2}{\epsilon_0 v_F}$$

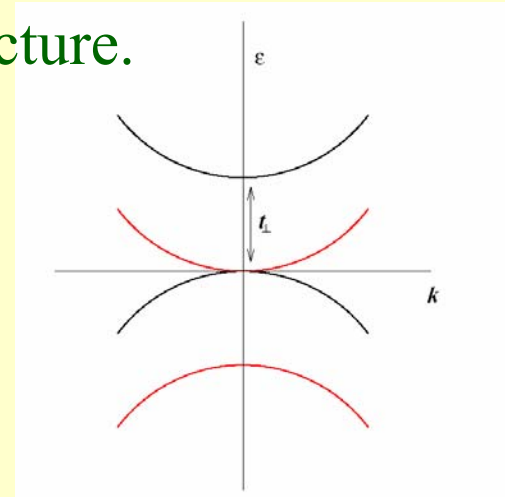
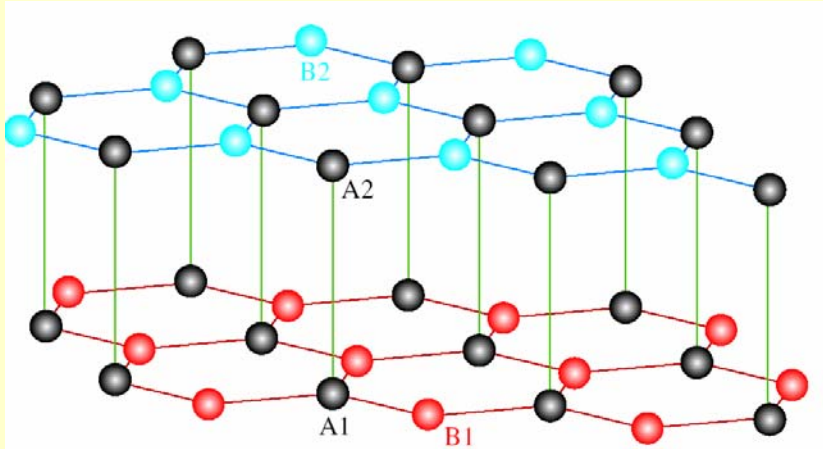
The instability is enhanced in the presence of disorder (neglecting localized states).

$$g_c \approx 3.8$$

The graphene bilayer.

E. McCann and V. Fal'ko, Phys. Rev. Lett. **96**, 086805 (2006)

Bilayer. Electronic structure.

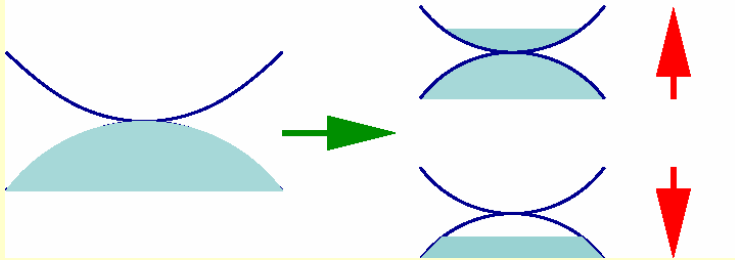


$$H \equiv \begin{pmatrix} 0 & v_F(k_x + ik_y) & 0 & 0 \\ v_F(k_x - ik_y) & 0 & t_{\perp} & 0 \\ 0 & t_{\perp} & 0 & v_F(k_x - ik_y) \\ 0 & 0 & v_F(k_x + ik_y) & 0 \end{pmatrix}$$

$$\mathcal{E}_{\vec{k}} \approx \frac{v_F^2 |\vec{k}|^2}{t_{\perp}}$$

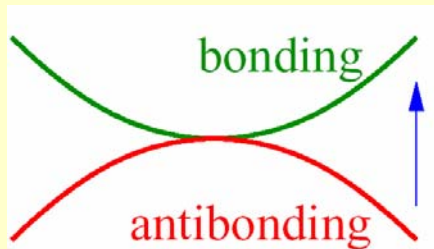
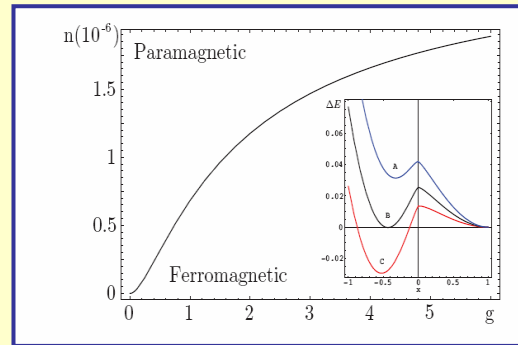
The graphene bilayer.

J. Nilsson, A. H. Castro Neto, N. M. R. Peres, and F. G. Phys. Rev. B 73, 214418 (2006)



The intraband exchange energy increases.
 The interband energy (proportional to the overlap between spinors) decreases.
 The problem resembles closely a dilute 2DEG.

Long range exchange interaction: $\frac{E}{S} = \frac{E_{kin} + E_{ex}}{S} \approx \frac{Q^4}{8\pi\pi_{\perp}} - \frac{2gQ^3}{27\pi^3}$ \longrightarrow Ferromagnetism



$$\chi_{AFM}^0(\vec{q}, \omega) \approx \int \frac{d^2k}{\omega - |\vec{k} + \vec{q}|^2/t_{\perp} + |\vec{k}|^2/t_{\perp}} \approx \log\left(\frac{t_{\perp}}{\omega - |\vec{q}|^2/4t_{\perp}}\right)$$

Short range Hubbard repulsion: \longrightarrow Antiferromagnetism

Similar effects expected in bulk graphite

Graphene multilayers.

Electronic structure and stacking order.

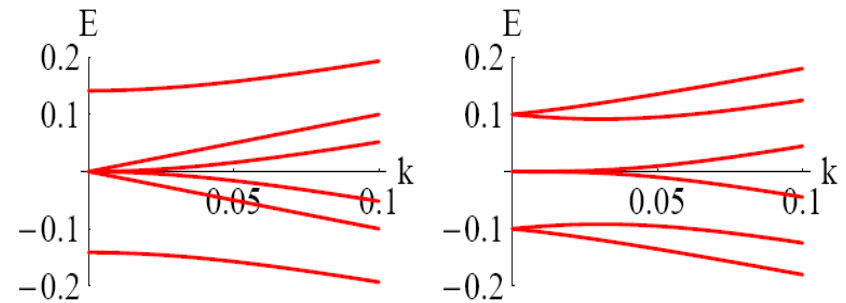
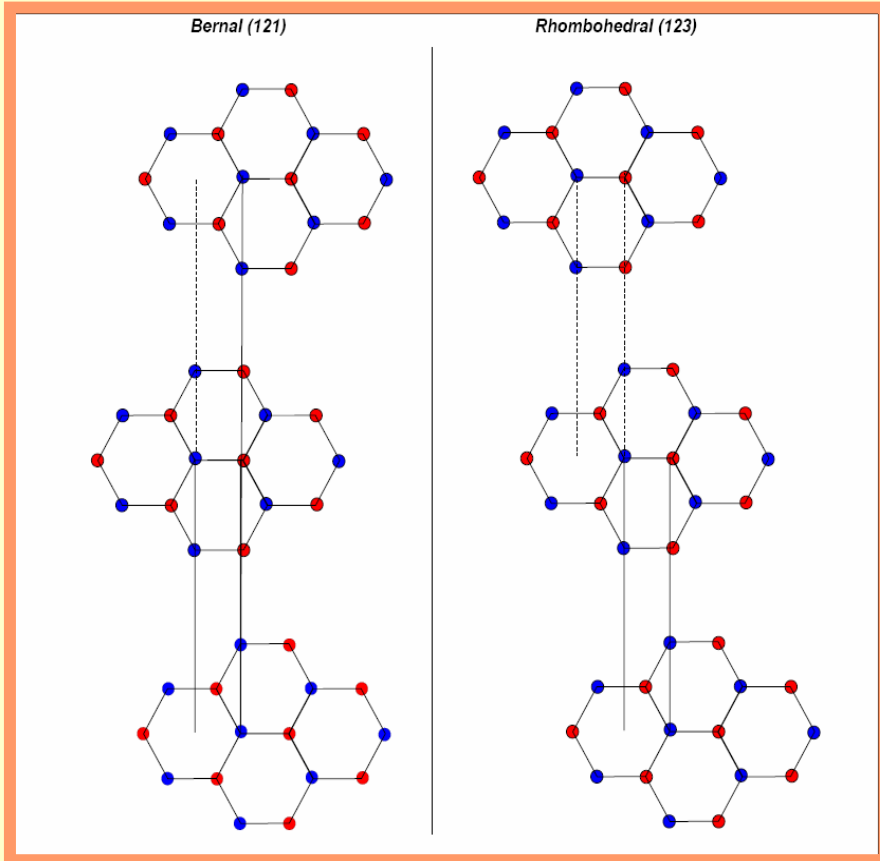
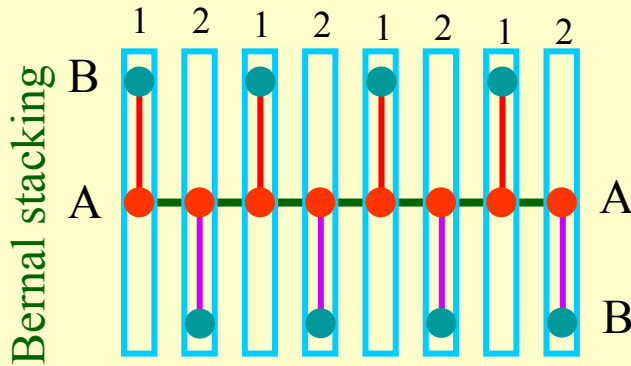


FIG. 1: Electronic structure of a trilayer. Parameters: $t_{\perp} = 0.1$, $v_F = 1$. Left: Bernal stacking, (121). Right: Rhombohedral stacking: (123).

- The bands of a trilayer with Bernal stacking are equivalent to those of a bilayer and a single layer superimposed.
- The bands of a bilayer with rhombohedral stacking show an incipient surface state.

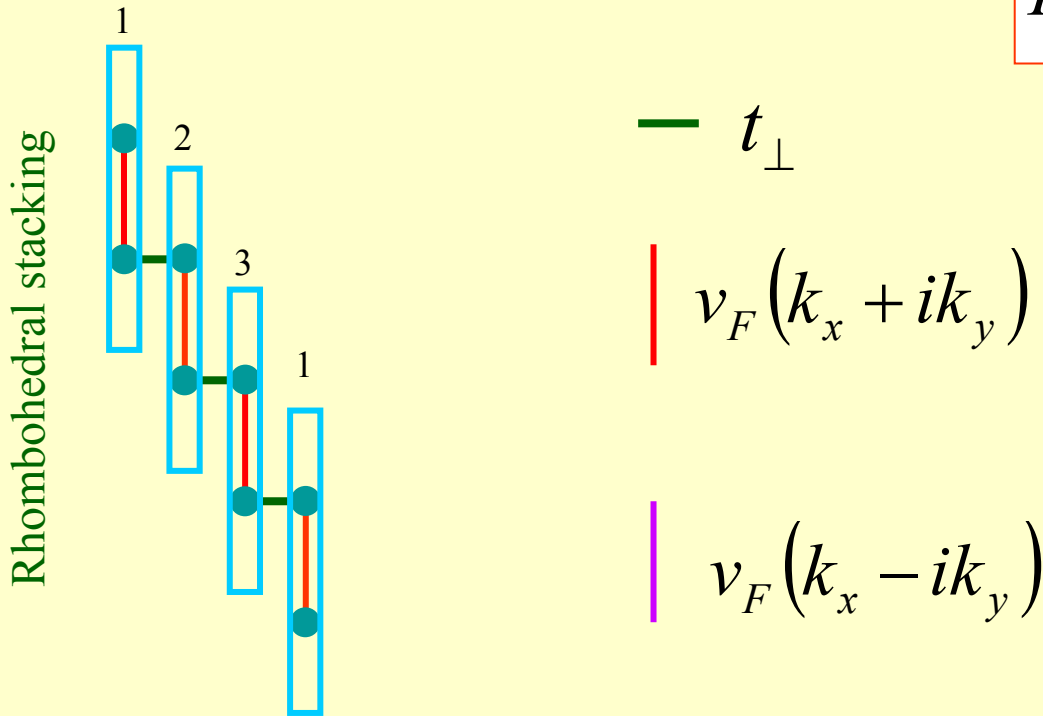
Graphene multilayers.

Effective hamiltonian.



The hamiltonian for each value of the parallel momentum defines a one dimensional tight binding model.

$$H \equiv \sum H_{k_{\parallel}}(t_{\perp}, v_F)$$



Graphene multilayers.

Bulk and surface density of states.

GUINEA, CASTRO NETO, AND PERES

PHYSICAL REVIEW B 73, 245426 (2006)

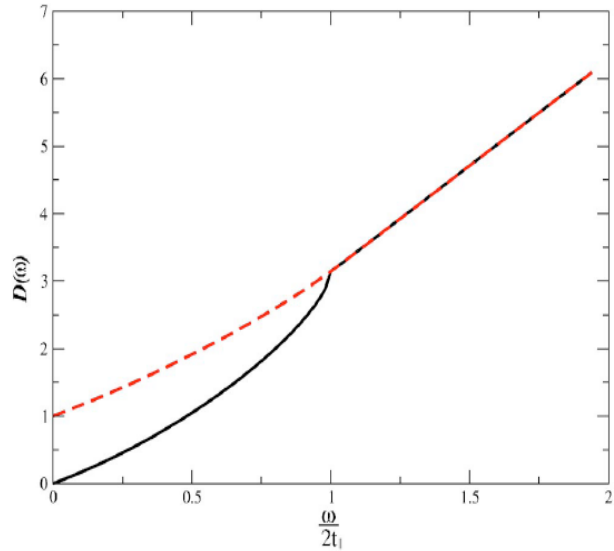


FIG. 5. (Color online) Density of states for the staggered stacking. Continuous line, $\text{Im } G_B(\omega)$. Dashed line, $\text{Im } G_A(\omega)$.

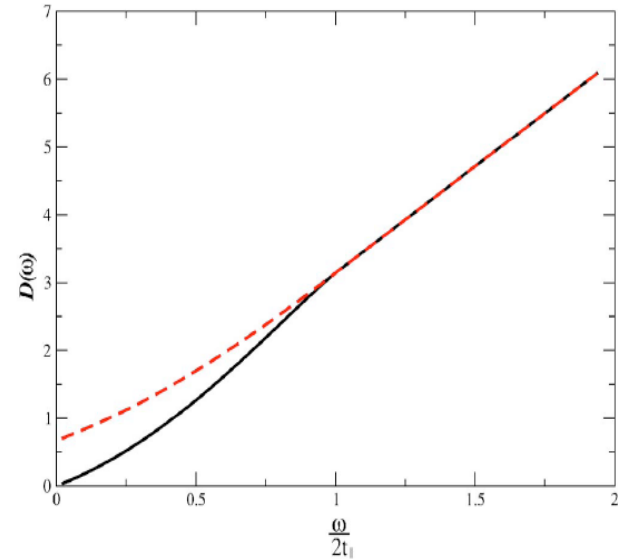


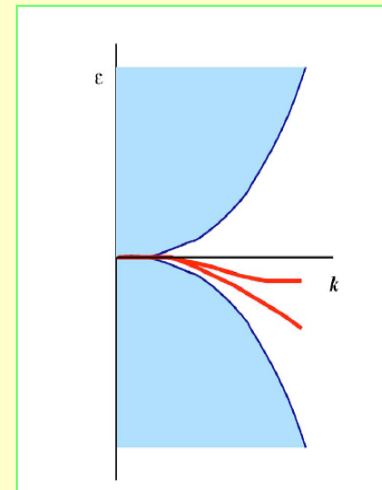
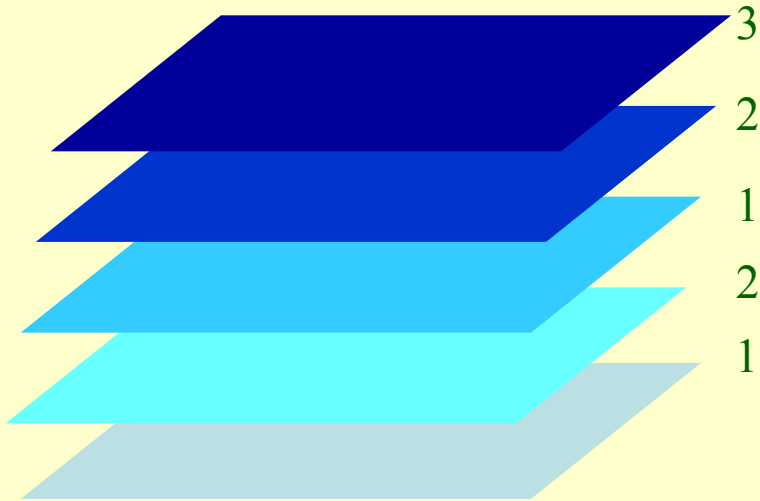
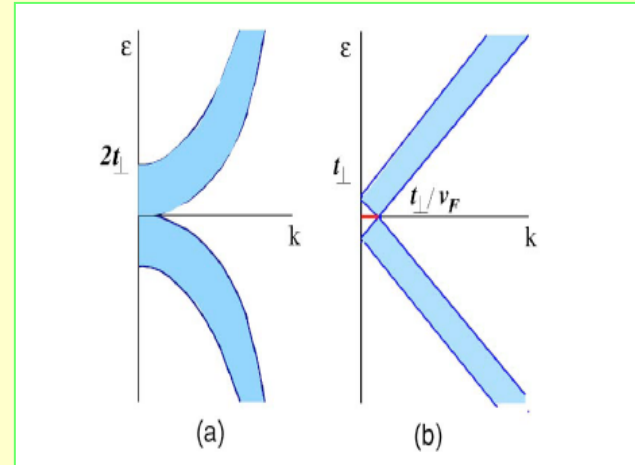
FIG. 6. (Color online) Density of states at the surface layer. Continuous line, $\text{Im } G_B(\omega)$. Dashed line, $\text{Im } G_A(\omega)$.

The low energy electronic states have vanishing amplitude on the atoms connected to the neighboring layers.

Graphene multilayers.

Surface states.

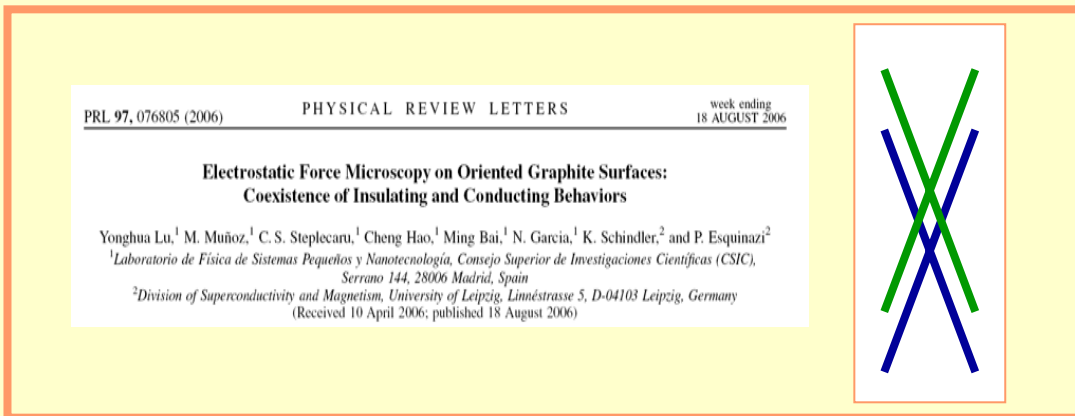
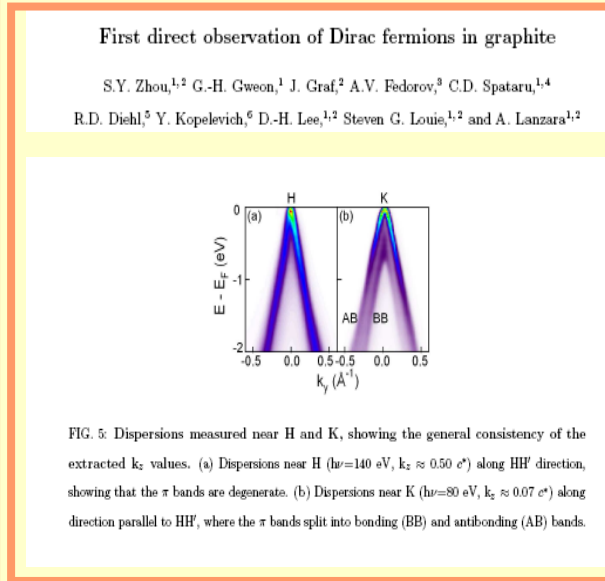
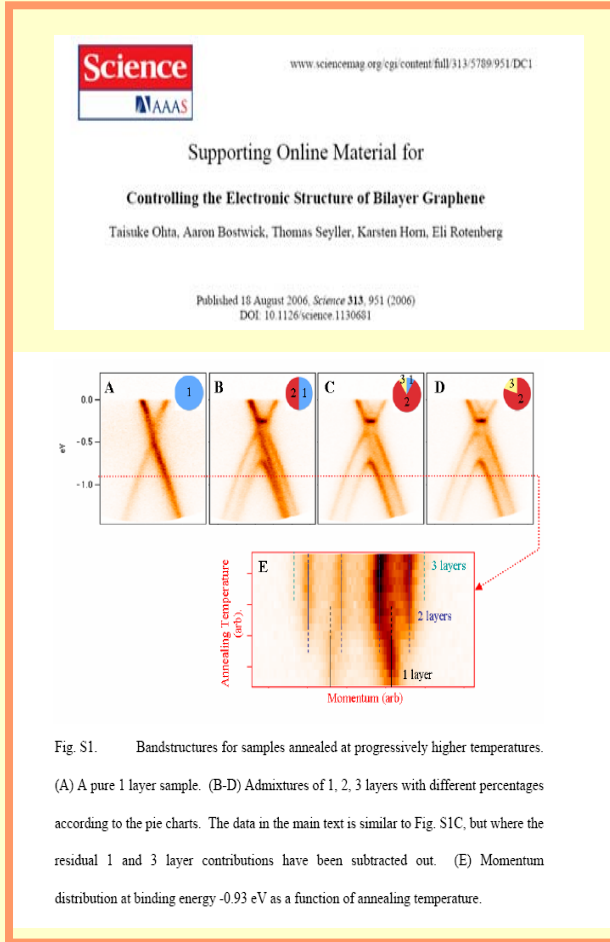
- Projected density of states:
 - Bernal stacking (121212...)
 - Rhombohedral stacking (123123...)



- Surface states can be induced near stacking defects.

Graphene multilayers.

Some experimental results.

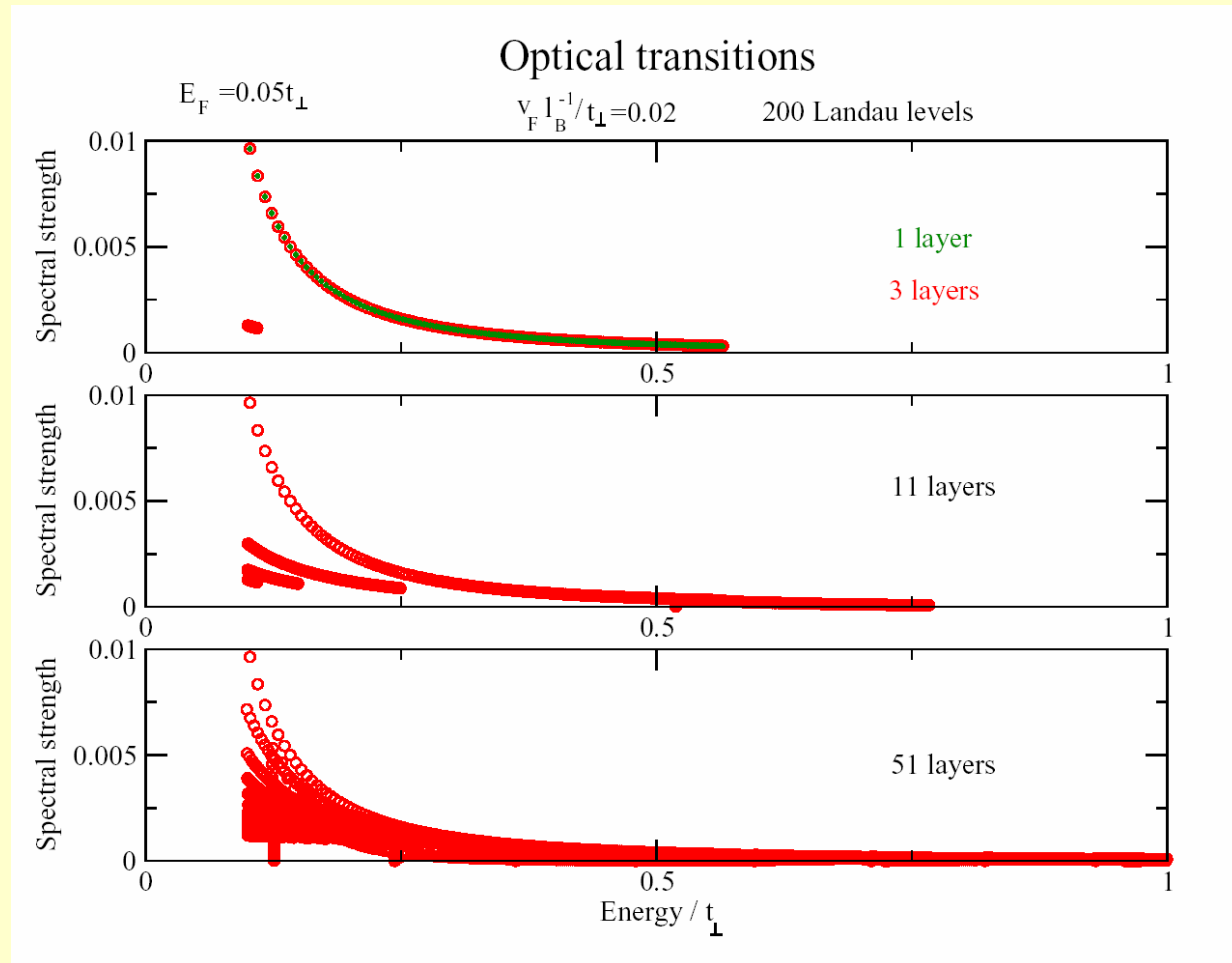


Conductance channels. Graphene multilayers.

N. M. R. Peres, A. H. Castro Neto and F. G., Phys. Rev. B **73**, 195411 (2006)

N. M. R. Peres, A. H. Castro Neto, and F. G., Phys. Rev. B **73**, 241403 (2006).

F. G., A. H. Castro Neto and N. M. R. Peres, Phys. Rev. B **73**, 245426 (2006), and to be published.

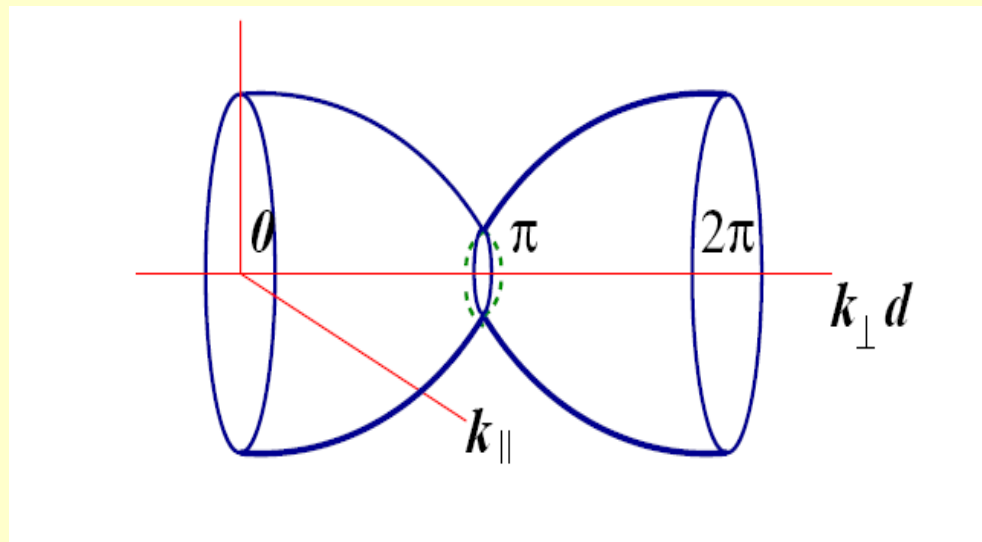


Landau levels associated to the Dirac equation can be observed in multilayers, or for special stackings, 123123123...

Graphene multilayers.

I. A. Luk'vanchuk and Y. Kopelevich, cond-mat/0609037, and Phys. Rev. Lett. **93**, 166402 (2004).

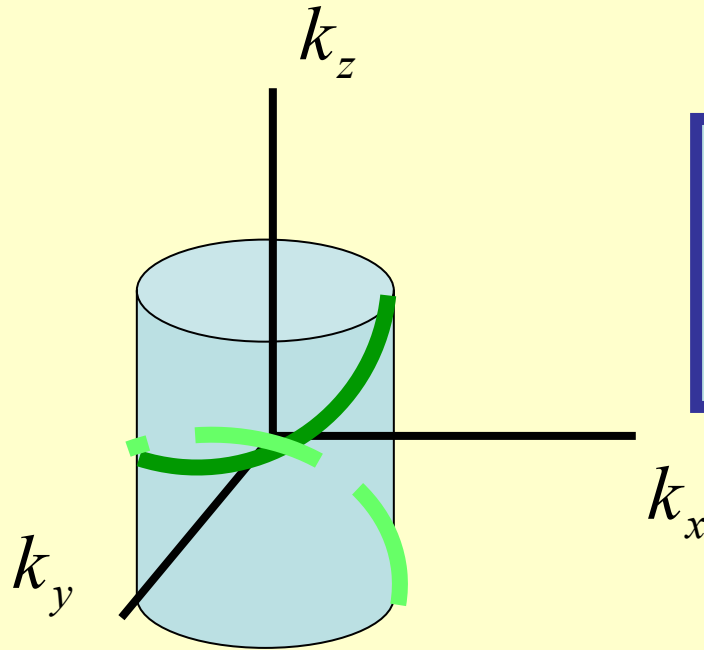
Fermi surface. Extremal orbits.



- The Fermi surface, to lowest approximation, contains a regular orbit, and a Dirac orbit.

Graphene multilayers.

Rhombohedral graphite.

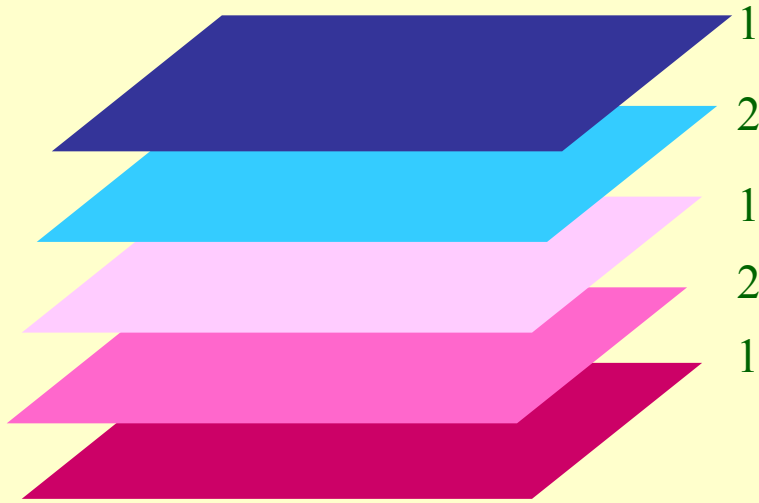


- The hamiltonian of rhombohedral graphite is made up of a set of Dirac equations, one for each value of k_z .
- There are surface states at the top and bottom layers of rhombohedral graphite.

$$H(k_{\parallel}, k_{\perp}) \equiv \begin{pmatrix} 0 & v_F(k_x + ik_y) + t_{\perp} e^{ik_z d} \\ v_F(k_x - ik_y) + t_{\perp} e^{-ik_z d} & 0 \end{pmatrix}$$

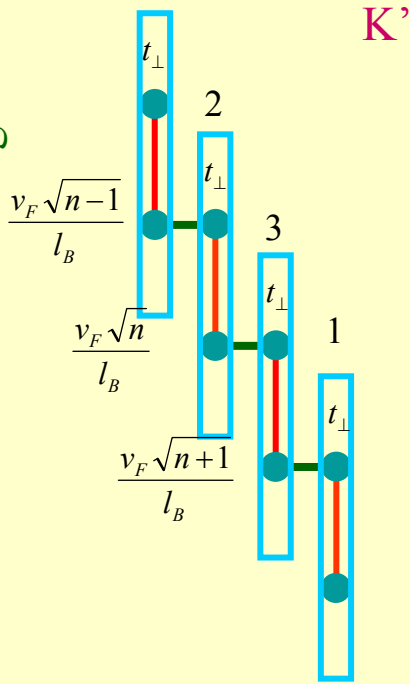
Graphene multilayers.

K Landau levels.



There is a $n=0$ Landau level derived from valley K at one surface, while the corresponding $n=0$ Landau level from valley K' is at the opposite surface (valley filtering).

Rhombohedral stacking



$$\begin{aligned}\varepsilon_m a_n &= t_{\perp} a_{n-1} + \frac{v_F \sqrt{n}}{l_B} a_{n+1} \\ \varepsilon_m a_{n-1} &= t_{\perp} a_{n-2} + \frac{v_F \sqrt{n}}{l_B} a_n \\ \varepsilon_m a_{n-2} &= t_{\perp} a_{n-1} + \frac{v_F \sqrt{n-1}}{l_B} a_{n-1} \\ \dots\end{aligned}$$

$$\varepsilon_m = \frac{v_F \sqrt{m}}{l_B}$$

The Landau levels in a rhombohedral stack are quasi two dimensional.

Graphene multilayers.

Rhombohedral stacking. Landau levels.

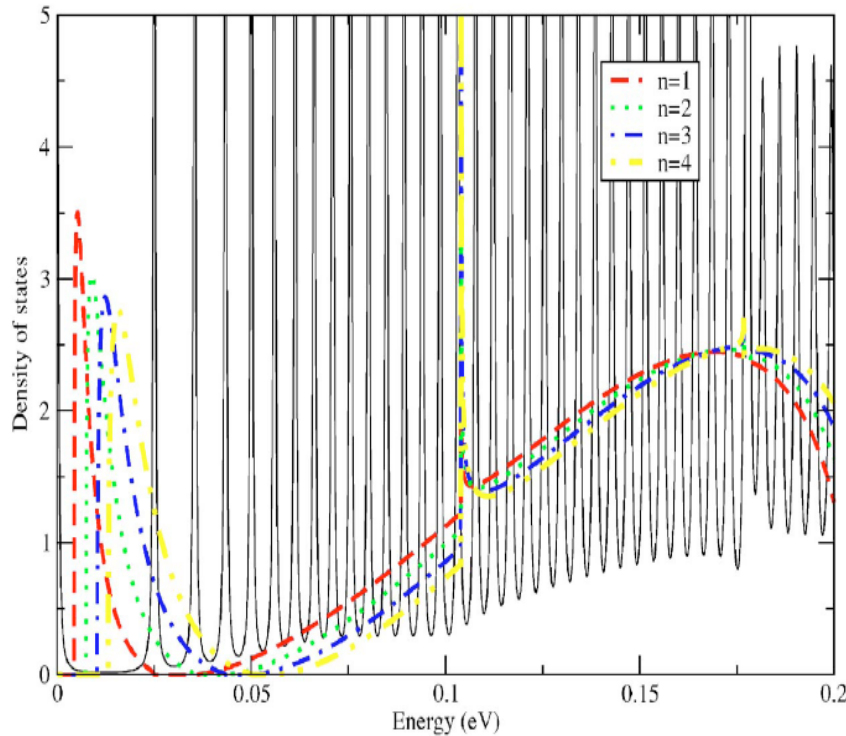


FIG. 7. (Color online) Average density of states of a stack of 50 graphene layers with rhombohedral order, 1-2-3-1-2-3 \dots , embedded into the staggered stacking, 1-2-1-2 \dots . The parameters used are $t_{\perp}=0.1$ eV, and $B=1$ T ($\ell_B \approx 25.7$ nm, $v_F/\ell_B \approx 0.025$ eV). The bands of some of the lowest Landau levels of the staggered stacking, calculated for the same parameters, are shown for comparison.

- The Landau levels of rhombohedral graphite are quasi two dimensional.

Graphene multilayers.

Disorder. Conductivity.

J. Nilsson, A. H. Castro Neto, F. G., and N. M. R. Peres, cond-mat/0604106

$$J_{\perp} = -2ed \sum_{k_{\parallel}} \sin(k_{\perp}) \left(c_{A_1 k_{\parallel}}^+ c_{A_2 k_{\parallel}} + c_{A_2 k_{\parallel}}^+ c_{A_1 k_{\parallel}} \right)$$

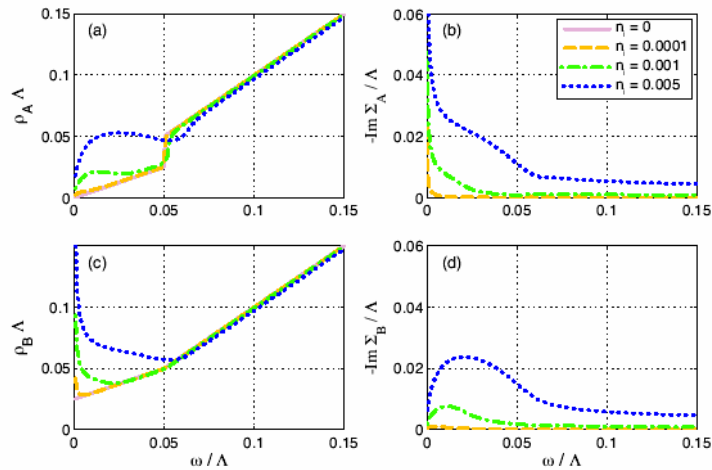


FIG. 1: (Color online) Bilayer DOS and self-energy (in units of the Λ) in the CPA approximation. DOS on the A(a) and B(c) sublattice as a function of the frequency (in units of Λ), imaginary part of the self-energy on the A(b) and B(d) sublattice as a function of the frequency.

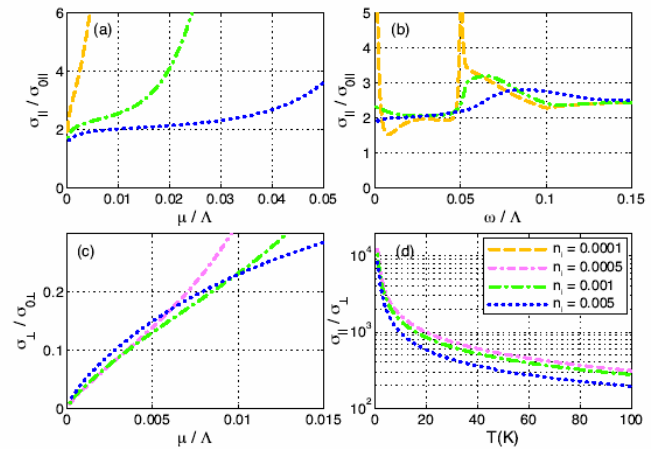


FIG. 4: (Color online) (a) In-plane DC conductivity in the bilayer as a function of the chemical potential (in units of Λ). (b) In-plane conductivity in the bilayer as a function of frequency at $T = 300\text{K}$ and $\mu = 0$ (in units of Λ). (c) Perpendicular DC conductivity in the multilayer as a function of the chemical potential (in units of Λ). (d) Anisotropy ($\sigma_{\parallel}/\sigma_{\perp}$) of the DC conductivity in the multilayer as a function of the temperature (in K) at $\mu = 0$.

The out of plane current requires the passage of the electrons through atoms with a semimetallic density of states.

- The in plane conductivity saturates at a value independent of the number of carriers.
- The out of plane conductivity is insulating.

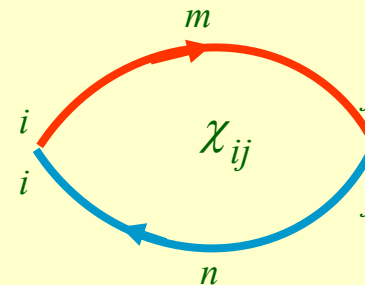
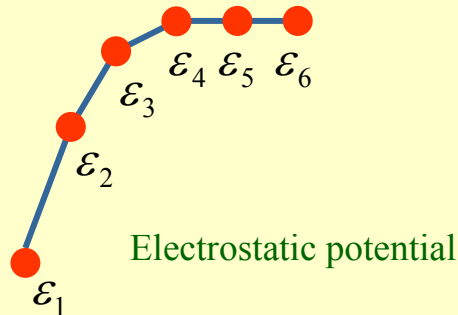
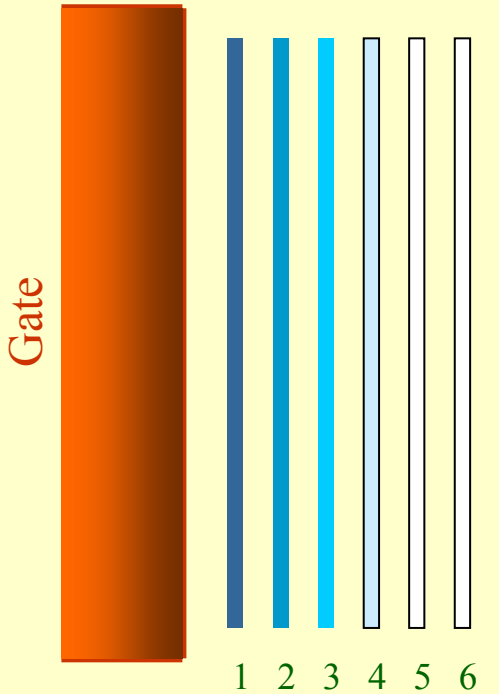
Graphene multilayers.

Induced charge at surfaces.

See also E. McCann, [cond-mat/0608221](#)

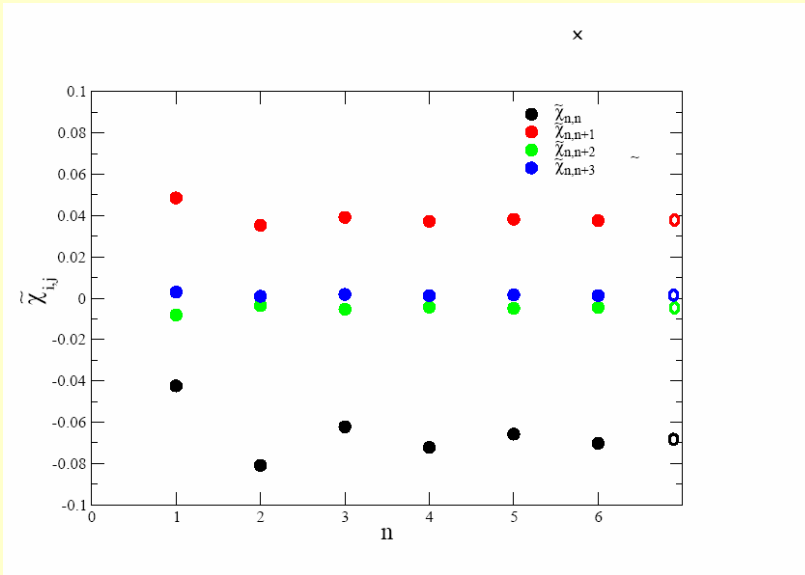
- The potential has to be calculated self consistently.
- The induced charge is calculated within linear response theory (RPA).

$$\begin{aligned}\varepsilon_i &= \varepsilon_{i-1} + e^2 d \sum_{j=1}^{i-1} n_j \\ \varepsilon_{i+1} - 2\varepsilon_i + \varepsilon_{i-1} &= e^2 d n_i \\ n_i &= \sum_j \chi_{ij} \varepsilon_j\end{aligned}$$



Graphene multilayers.

Induced charge at surfaces.



The decay of the charge into the bulk can be calculated analytically:

$$\varepsilon_i = \varepsilon_0 e^{-n\kappa}$$

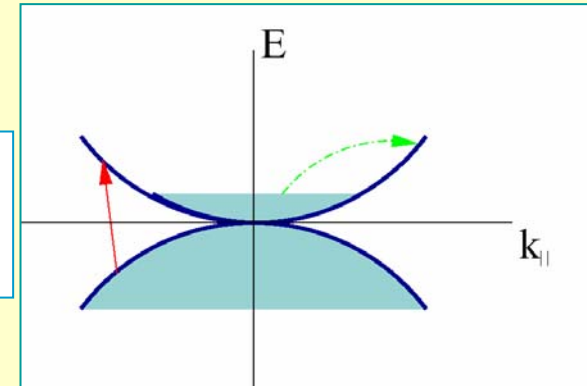
$$n_i = n_0 e^{-n\kappa}$$

$$e^\kappa - 2 + e^{-\kappa} = e^2 d \sum_{n=-\infty}^{n=\infty} e^{-|n|\kappa} \chi_n^{bulk} =$$

$$= \frac{4e^2 dt_\perp}{\pi^3 v_F^2} \log\left(\frac{t_\perp}{\varepsilon_0}\right) \int_{-\pi/2}^{\pi/2} d\phi \int_{\pi/2}^{3\pi/2} d\phi' \frac{\sinh(\kappa)}{\cosh(\kappa) - \cos(\phi - \phi')} \frac{\cos(\phi)\cos(\phi')}{\cos(\phi) - \cos(\phi')}$$

The charge polarizability has inter- and intraband contributions.

$$\chi_{ij} = \frac{4}{\pi} \frac{t_\perp}{v_F^2} \tilde{\chi}_{ij} \log\left(\frac{t_\perp}{\varepsilon_0}\right)$$



Intraband contribution at finite doping:

$$\kappa^2 \approx e^2 dD(\varepsilon_F) = \frac{4e^2 dt_\perp}{\pi^2 v_F^2} \approx 0.09$$

$$\frac{e^2}{v_F} \approx 1$$

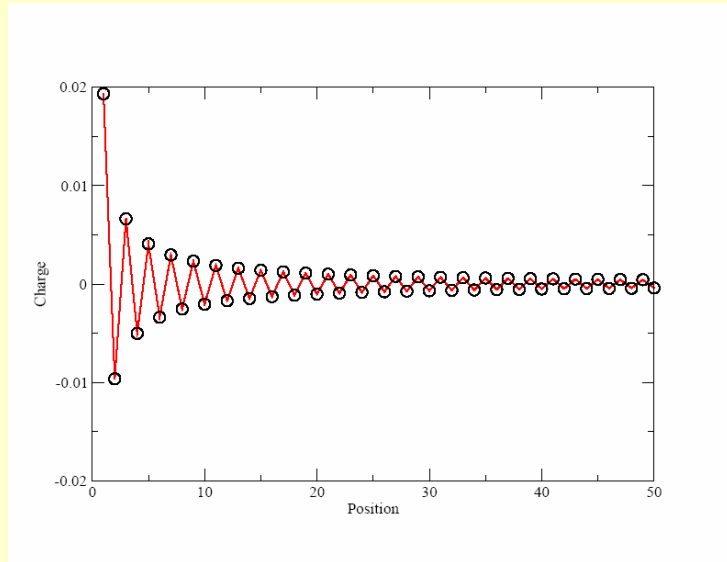
$$\frac{t_\perp d}{v_F} \approx \frac{1}{5}$$

$$\kappa^{-1} \approx N \approx 3-4$$

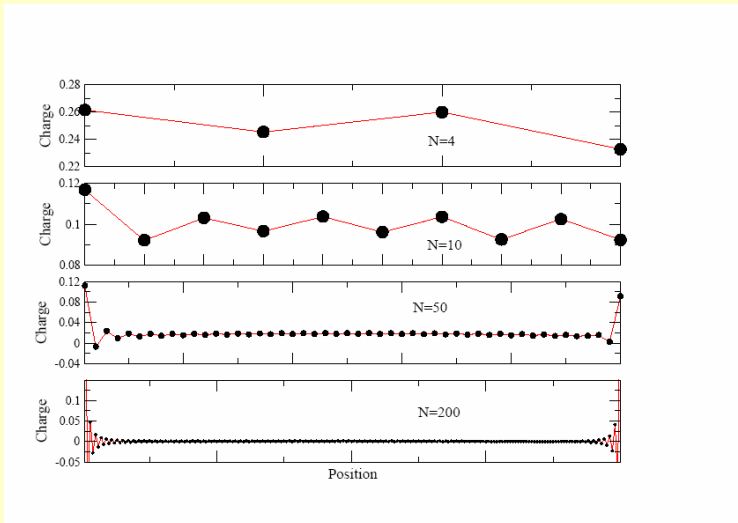
Interlayer transitions only lead to anomalous, quasi insulating screening.

Graphene multilayers.

Induced charge in multilayers.



The charge distribution near a neutral surface shows a slow decay, and oscillations with period equal to the interlayer distance.



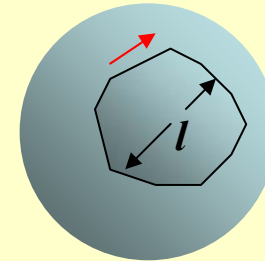
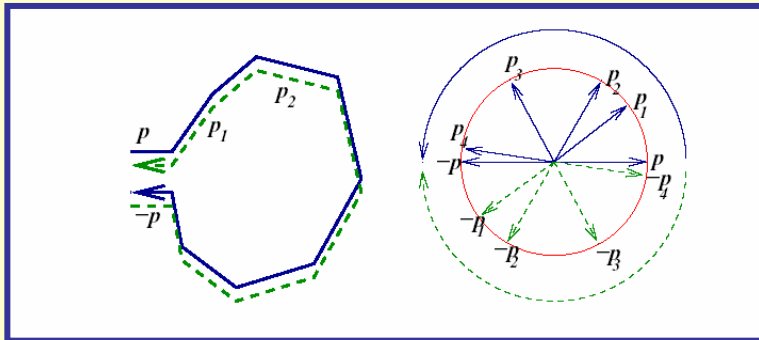
The charge oscillations persist in doped multilayers. Metallic screening localizes most of the charge within 3-4 layers.

Curvature and weak (anti)localization.

A. Morpurgo and F. G., cond-mat/0603789.

See also: S. V. Morozov, K. S. Novoselov, M. I. Katsnelson, F. Schedin, D. Jiang, and A. K. Geim, cond-mat/0603826
 E. McCann, .K. Kechedzhi, V. I. Fal'ko, H. Suzuura, T. Ando, and B. L. Altshuler, cond-mat/0604015

- Smooth disorder should lead to antilocalization effects in graphene, H. Suzuura and T. Ando, Phys. Rev. Lett. **89**, 266603 (2002).
- Neither localization nor antilocalization effects have been observed.



Antilocalization due to negative interference (Berry's phase).

On a curved surface, the accumulated rotation along a closed path is not π .

$$\varphi \approx \pi - c \left(\frac{l}{R} \right)^2$$

$$\frac{l}{R} \approx \frac{h}{l^2}$$

$$\delta\varphi \approx \sqrt{N} \left(\frac{h}{l} \right)^2 \approx \frac{Lh^2}{l^3}$$

Antilocalization effects disappear for:

$$l \approx 10 \text{ nm}$$

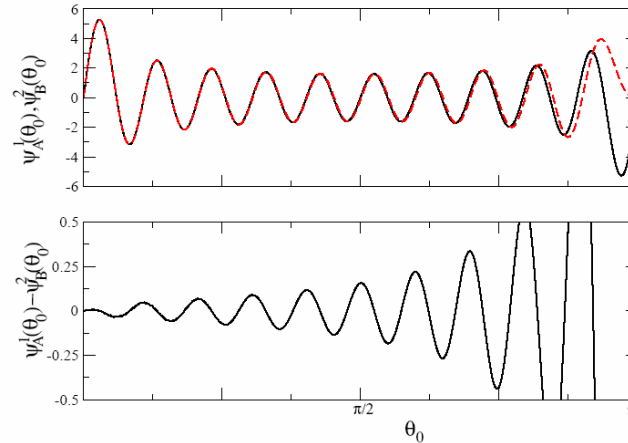
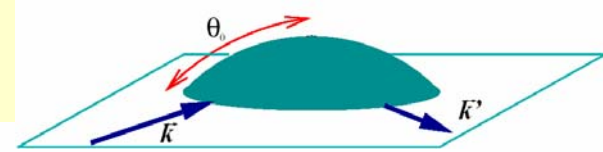
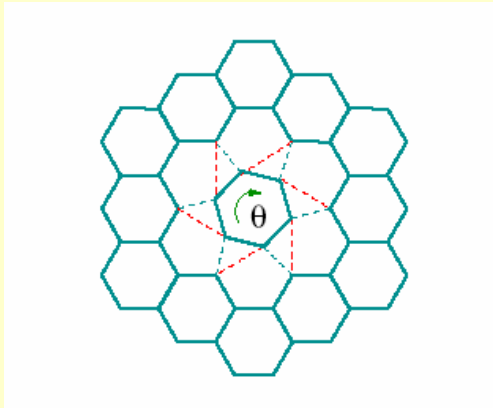
$$h \approx 1 \text{ nm}$$

$$L \approx 10^3 \text{ nm}$$

Curvature and weak (anti)localization.

Other effects.

F. G., J. González, and M. A. H. Vozmediano, Phys. Rev. B **59**, 134421 (2001)



Effective gauge field:

- Local rotations of the lattice axes.
- Topological defects: disclinations (pentagons, heptagons), dislocations.

Scattering at boundaries

M. V. Berry, and R. J. Mondragon, Proc. R. Soc. Lond. A **412**, 53 (1987).

$$\tau_{gauge}^{-1} \approx \frac{v_F}{\sqrt{k_F^{-1} d}}$$

d : distance between dislocations.

Inequivalence between sublattices (mass term).

Conclusions

- Interaction effects can be important in multilayered systems.
- The electronic structure depends on the stacking order. Valley filtering occurs in a magnetic field.
- Quasi two dimensional behavior can be found when stacking defects are present.

J. Nilsson, A. H. Castro Neto, N. M. R. Peres, and F. G. Phys. Rev. B **73**, 214418 (2006)
F. G., A. H. Castro Neto and N. M. R. Peres, Phys. Rev. B **73**, 245426 (2006)
J. Nilsson, A. H. Castro Neto, F. G., and N. M. R. Peres, cond-mat/0604106

- Undoped graphite surfaces can show insulating behavior.
- Induced charge has oscillations from layer to layer.
- Screening in doped multilayers leads to a charge distribution localized in 3-4 layers.

- Diffusion in curved surfaces suppress weak antilocalization effects.

A. Morpurgo and F. G., cond-mat/0603789.